LAWRENCE
LIVERMORE
NATIONAL
LABORATORY

UCRL-JRNL-234567

Coda Spectral Peaking for Nevada Nuclear Test Site Explosions

K. R. Murphy, K. Mayeda, W. R. Walter

September 12, 2007

Bulletin of the Seismological Society of America

Coda Spectral Peaking for Nevada Nuclear Test Site Explosions

K. R. Murphy, K. Mayeda, W. R. Walter

ABSTRACT

We have applied the regional *S*-wave coda calibration technique of *Mayeda et al*. (2003) to earthquake data in and around the Nevada Test Site (NTS) using 4 regional broadband stations from the LLNL seismic network. We applied the same path and site corrections to tamped nuclear explosion data and averaged the source spectra over the four stations. Narrowband coda amplitudes from the spectra were then regressed against inferred yield based on the regional m_b(*Pn*) magnitude of *Denny et al*. (1987), along with the yield formulation of *Vergino and Mensing* (1990). We find the following: 1) The coda-derived spectra show a peak which is dependent upon emplacement depth, not event size; 2) Source size estimates are stable for the coda and show a dependence upon the near-source strength and gas porosity; 3) For explosions with the same m_b(*Pn*) or inferred yield, those in weaker material have lower coda amplitudes at 1-3 Hz.

INTRODUCTION

Explosions and shallow-depth earthquakes have a distinctive coda spectral shape relative to normal depth earthquakes, consisting of a low-frequency "peak" or bump (*Mayeda and Walter*, 1996, *Myers et al*., 1999). While the origin of the bump in the explosion spectra appears to be consistent with *Rg*-to-*S* scattering (*Myers et al*., 1999), the factors controlling the frequency of the bump's peak have not been investigated before. In this study, we look at source size (explosion yield), spall, and depth as controls on the frequency at which the coda spectral peak occurs. As official explosion yields have not been publicly released for most NTS tests, all references to yield in this paper

are estimates using the amplitude of the Pn phase in the $m_b(Pn)$ from *Denny et al.* (1987) and the $m_b(Pn)$-yield relationship of *Vergino and Mensing* (1990). We find the frequency of the coda spectral peak is a function of source emplacement depth and not event spall or size. This is a useful result because source depth is an important tool for discrimination between earthquakes and explosions. For regions that are well-calibrated, the location of the spectral peak might be used to identify very shallow events and provide a quantitative estimate of the source depth.

It has been demonstrated that narrowband regional *Lg*-coda amplitudes can provide reliable estimates of m_b (e.g., *Mayeda*, 1993), and more recently, that they can be used to derive stable source spectra and single-station estimates of M_w (*Mayeda et al*., 2003). The scattering properties of seismic coda minimize source radiation and directivity effects, providing more stable estimates of magnitude than direct phases. This property of coda waves is especially useful when a magnitude is needed from a very sparse network. In this study, we calibrate the Nevada Test Site (NTS) region using earthquakes in and around NTS, and then apply the same path and site corrections to the explosion data.

Several authors have studied the source of *S* and *Lg* waves in underground explosions, and determined that *Lg* can be generated by *Rg*-to-*S* scattering near the source (e.g. *Patton and Taylor*, 1995, *Gupta et al*., 1992), while others attribute explosion shear waves to source-generated *S*, trapped *pS* (e.g. *Stevens et al*., 2006, *Stevens et al*., 2007), scattering due to topography and near-source complexity (e.g. *Myers et al*., 2006; *Myers*, 2007), and crack growth (e.g. *Sammis et al*., 2007). *Mayeda and Walter* (1996) hypothesized that *Rg* scattering into the coda caused a peak in the coda spectra of explosion and shallow-source earthquakes, in contrast to normal depth crustal earthquakes. In a study of the 1997 Kazakhstan depth of burial experiment, *Myers et al*.

(1999) noted that *Rg* was the largest arrival at distances smaller than 10 km, but it scattered or attenuated so rapidly that it was not seen at regional distances. At local distances, an *Rg* spectral peak at 1-5 Hz was observed. At further distances, as *Rg* was scattered or attenuated, the peak shifted to lower frequencies until it was no longer present. Interestingly, the regional coda spectra showed a peak also at about 1-5 Hz, leading the authors to suggest that *Rg* energy was being scattered into the coda at local distances. We believe this same phenomenon is responsible for the coda spectral peak we see in the NTS explosions.

Given the uncertainty and complexity in how explosions produce S-waves, it is remarkable that they have proven to be a very good predictor of source size or yield (e.g. *Nuttli*, 1986; *Patton*, 1988; *Mayeda*, 1993). For NTS explosions, the low frequency S-wave coda is affected by depth dependent spectral peaking and at high frequencies by source material properties. In the first part of this paper, we quantify the coda spectral peaking as a function of absolute depth. In the second part, we look at the stability of coda based measurements of source size by regressing *Lg* coda amplitudes against $m_b(Pn)$ using the inferred yield corrections of *Vergino and Mensing* (1990).

NARROWBAND CODA METHOD

A thorough description of the coda method can be found in *Mayeda et al*. (2003), so we only give a brief summary here. The coda method has been shown to be transportable to different tectonic environments, with each new area being calibrated to nearby earthquakes before explosions are analyzed. Using a set of calibration earthquakes, we deconvolve to velocity and form narrowband coda envelopes, measure the velocity of the envelope peak, measure coda shape parameters, generate synthetic envelopes, measure coda envelope amplitudes, and grid search for path correction

parameters (see *Mayeda et al*., 2003 for detailed processing steps). The distance-corrected amplitudes are then tied to an absolute scale using independently derived seismic moment estimates from waveform modeling. This last step corrects for the *S*-to-coda transfer function as well as the frequency-dependent site effects. The path and site corrections are then applied to the entire dataset and source spectra are averaged over the stations in the network. Once the coda amplitude calibration has been established from earthquakes, we can create coda envelopes for explosions using the same amplitude correction to produce stable spectra for each event. In this paper, we examine the coda-derived spectra for NTS explosions, and relate their amplitudes to inferred yield (*Vergino and Mensing*, 1990).

We apply the coda method described above to 188 NTS nuclear explosions from years 1969-1992, recorded at the four stations of the Lawrence Livermore National Lab (LLNL) seismic network. The area is calibrated using 23 NTS earthquakes. Figure 1 shows a map of the NTS explosions, earthquakes, and stations used in this study.

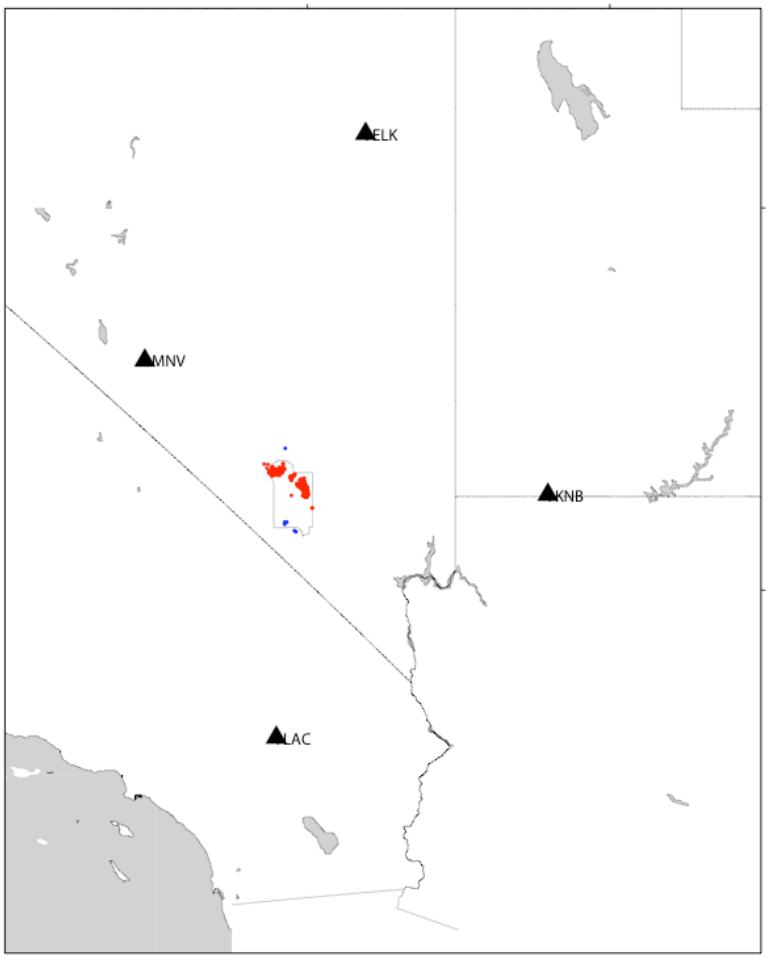

Figure 1. Map of the southwestern United States showing the stations used in this study (triangles), explosions (red dots), and earthquakes (blue dots). Polygon shows the bounds of the NTS region.

SPECTRAL PEAK

Following the calibration procedure, Figure 2a shows example earthquake source spectra for a range of events from the NTS region. We note that independent seismic moments (*W. Walter* and *G. Ichinose*, personal communication, 2007) are in good agreement with our estimates. In Figure 2b, we plot example spectra for six NTS explosions, each exhibiting a characteristic spectral peak or bump. Our focus is on which factor controls the spectral peak frequency. In general, larger yield explosions are buried deeper for containment, so it is unclear whether our observed spectral peak is a result of yield or depth. It has been proposed by *Myers et al.* (1999) that *Rg*-to-*S* scattering

redistributes the energy into the coda, causing a spectral peak that is dependent upon the depth of burial.

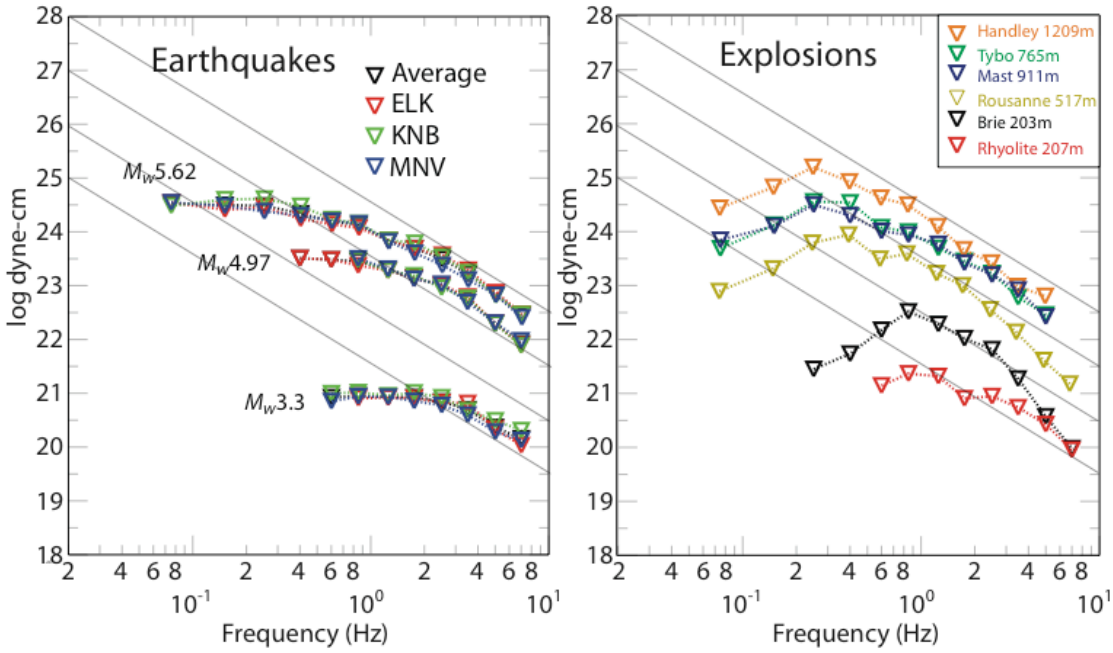

Figure 2. Example spectra from NTS earthquakes and explosions. 2A. (Left) Examples of earthquake spectra from our dataset exhibit the familiar shape. 2B. (Right) Explosion spectra have a "peak" not seen in earthquake spectra. The spectral peak is attributed to *Rg*-to-*S* scattering, and the frequency of the peak is a function of depth (*Myers et al*., 1999). Gas porosity controls the high frequency falloff rate.

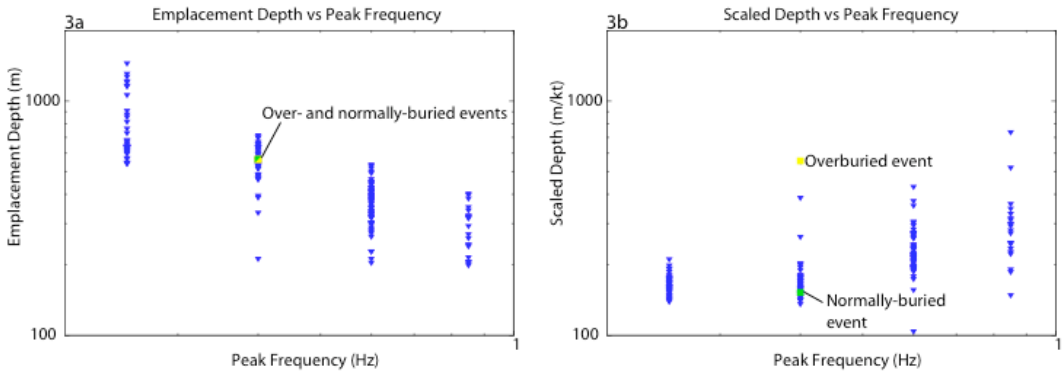

Figure 3. Spectral peak frequency vs emplacement depth (3a) and scaled depth (3b) for NTS explosions. There is a correlation between frequency of the spectral peak and emplacement depth, but not with scaled depth. This is evidence that the bump in the spectra is a result of emplacement depth. A correlation between peak frequency and scaled depth would suggest that spall controls the peak frequency. We highlight two explosions that have different seismic inferred yields but the same emplacement depth, resulting in one being overburied. Note that they plot together in the emplacement depth figure (3a), but are quite far apart in the scaled depth figure (3b).

As a first-order test, we plot the frequency of the spectral peak (e.g. Figure 2b) against two measures of depth: emplacement depth and scaled depth (Figure 3). Scaled depth, d_s, is the depth scaled for yield:

$$d_s = \frac{d}{Y^{0.295}},$$

where d is emplacement depth in meters, and Y is the seismic inferred yield in kilotons (Nordyke, 1962). Here, we calculate an inferred value for yield (*Vergino and Mensing*, 1990), which will be described in detail later in the paper. If the spectral peak is related to either spall or yield, we would expect to see a correlation between scaled depth and spectral peak frequency, since scaled depth is a function of yield. However, the spectral peak frequency does not correlate with scaled depth; rather, it correlates with emplacement depth. This result indicates to us that the spectral peak frequency is a function of absolute depth, not yield or spall.

For containment purposes, larger events are generally buried deeper than smaller ones, so it can be difficult to isolate the effects of yield and emplacement depth on the regional spectra. Fortunately, there are some overburied explosions that we can use for comparison, such as Borrego, which is adjacent to normally-buried Baseball, and has the same depth of ~564 meters (Figure 4). The event pair of Baseball and Borrego is interesting because the events' magnitudes differ by 1.7 units, which implies a large difference in their yields, yet their location and hence, near-source conditions, are virtually identical. Any differences between their spectral peak frequencies should be due to yield or spall, since other factors are constant (e.g., *Taylor and Randall,* 1989). Despite the large difference in seismic inferred yield, both events peak at 0.4 Hz, in agreement with our previous observation that spectral peak frequency correlates with depth (Figure 3a). There is not enough energy at low frequencies in the Borrego

spectrum for us to say that 0.4 Hz is its definitive peak, but we can say that the peak frequency for this event is not higher than 0.4 Hz, as would be expected if the peak were a function of source size.

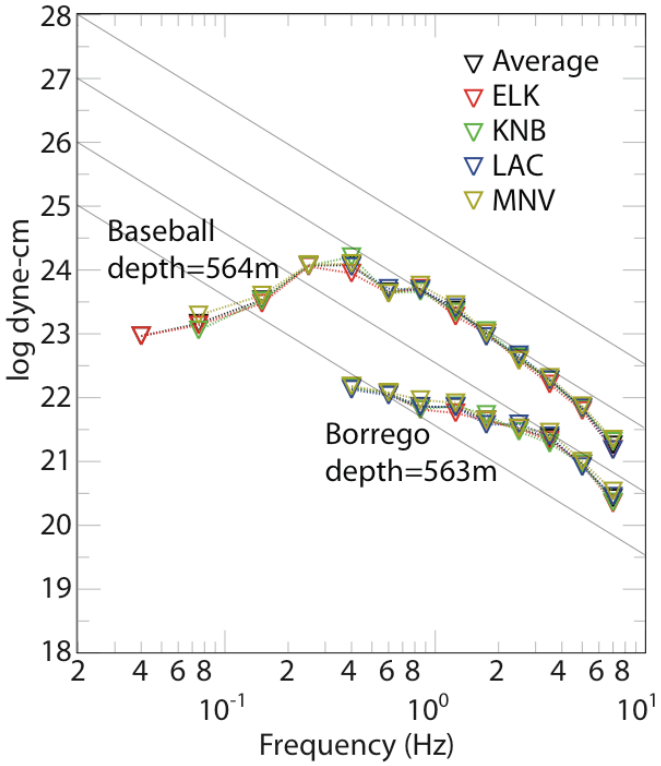

Figure 4. *Lg*-coda-derived source spectra of Baseball and Borrego, which share the same near-source material property and the same emplacement depth. However, they have very different seismic inferred yields. They both have a spectral peak in the 0.3-0.5 Hz band, indicating that the peak is more dependent on depth than yield (e.g., Figure 3b).

In addition to the spectral peak in the coda-derived spectra, the explosion spectra exhibit variable rate of high frequency falloff. For the direct phases (e.g., *Pg* and *Lg*) *Walter et al*. (1995) noted a correlation between spectral ratio and near-source material strength and gas porosity. Our data show a similar trend. In Figure 2, the three largest events, Handley, Tybo, and Mast, are in the high-strength volcanics of Pahute Mesa, in the northwestern part of NTS, and their high frequencies fall off as omega-squared. The smaller events, Rousanne, Brie, and Rhyolite, are in low-strength, high gas-porosity Yucca Flat alluvium, and have a much steeper high-frequency falloff. In contrast, high-

frequency falloff of explosions in high-strength material tend to behave like earthquakes, following the omega-squared model. Events in weak material, however, fall off much more quickly, closer to omega-cubed or steeper. *Gupta et al*. (1992) found that high frequency *Lg* is dependent on the source medium velocity, and *Walter et al*. (1995) suggest that high-frequency falloff is a result of high gas porosity. Since gas porosity decreases with depth, high-frequency falloff rate may be useful for identifying shallow events, or as another earthquake/explosion discriminant (*Walter et al*., 1995). For sparse station monitoring, the coda spectral ratio may provide a more stable estimate of the high-frequency falloff rate than coda-derived spectra alone (e.g. *Mayeda et al.,* 2007).

RELATIONSHIP TO YIELD

Next, we investigate the scaling of *S*-wave coda envelope amplitudes with seismically inferred yield from $m_b(Pn)$. *Mayeda* (1993) examined magnitude-yield residuals for both $m_b(Lg\text{Coda})$ and $m_b(Pn)$. We use a similar approach, but our method differs in that we compare coda spectral amplitudes directly with seismic inferred yield, and separate the events into two groups based on the strength of the emplacement material.

To calculate inferred yield, we use *Vergino and Mensing's* (1990) $m_b(Pn)$ to yield relation:

$$\log y = \frac{m_b(Pn) - \hat{a}_R - \hat{c}Gp}{\hat{b}},$$

where $m_b(Pn)$ is calculated using the method of *Denny et al*. (1987), a_R is an intercept value, *Gp* is the gas-filled porosity, *c* is a measure of the dependence on *Gp* in percent, and *b* is the slope. The parameters a_R, *Gp*, *c*, and *b* are specific to one of four regions, based on gas-filled porosity, within NTS (See *Vergino and Mensing* (1990) for details). Finally, we regress the inferred yield values against the narrowband coda amplitudes.

Figure 5 shows the relationship between coda envelope amplitude and inferred yield for three frequency bands ranging between 1 and 3 Hz. We use this frequency band to avoid the spectral bumps discussed in the previous section. Events are separated by low strength source material (solid symbols) and high strength source material (open symbols), based on gas porosity and location relative to the water table. The criteria for separating into high and low strength material are the same as that used in *Walter et al*. (1995). The two material types have slightly different scaling relationships between coda amplitude and inferred yield. If coda amplitudes were to be used as an indicator of yield, it would be useful to have information about the emplacement conditions, in addition to what is known about the area from the original earthquake-based calibration. The curves in high-strength (low-gas porosity) material give a minimum bound on the seismic yield relative to more porous material; therefore, this yield estimate is more conservative. Given the importance of emplacement media to coda amplitude scaling, we may expect other test sites to be different (e.g., Lop Nor, Novaya Zemlya, Semipalitinsk, North Korea, India).

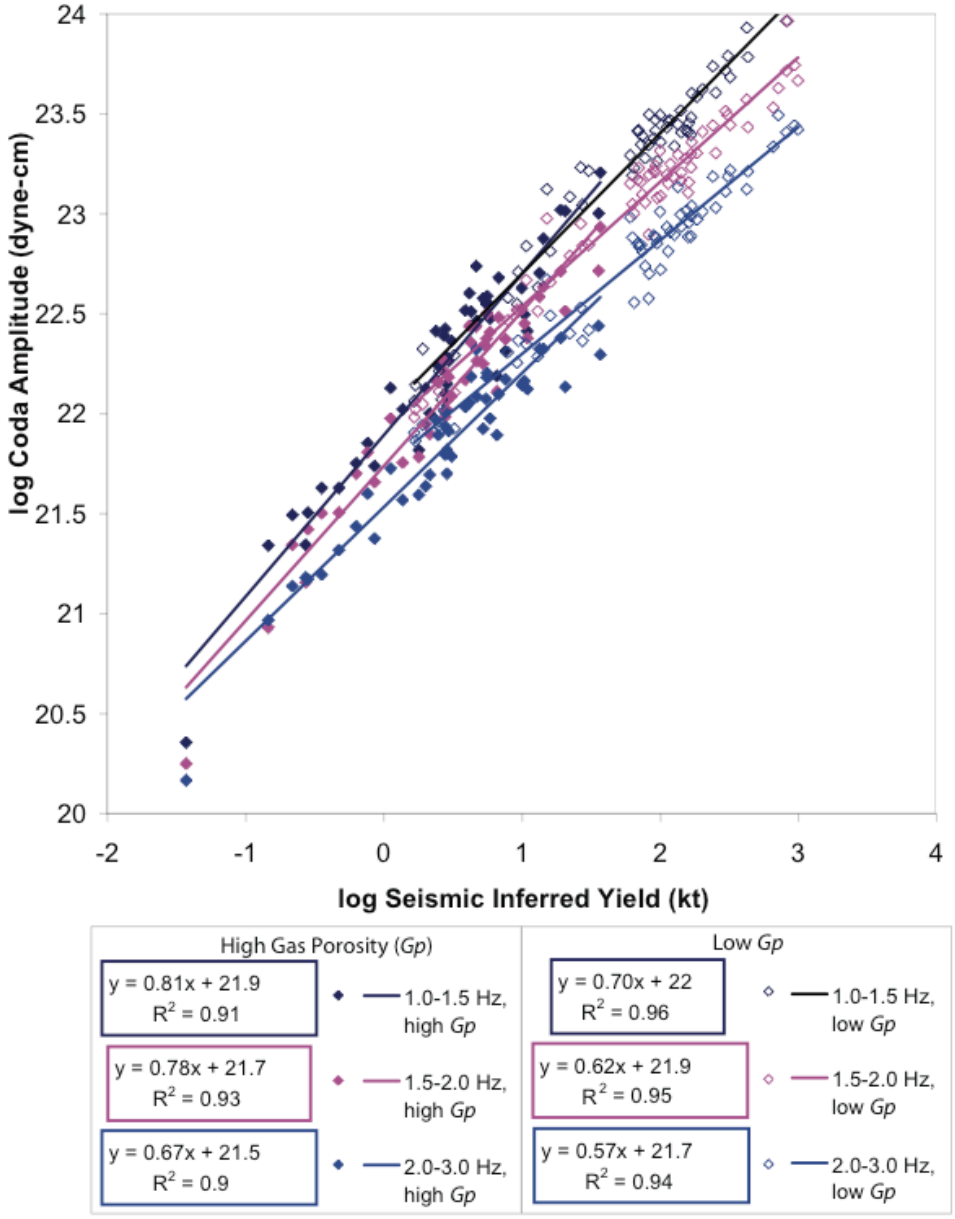

Figure 5. Inferred yield calculated from m_b(*Pn*) (Denny *et al*., 1987) using *Vergino and Mensing's* (1990) relation. The scaling relation between inferred yield and coda amplitude is dependent upon emplacement conditions. The smallest event is a very shallow explosion in very weak, high-gas porosity material.

DISCUSSION

The spectral bump (Figures 3 and 4) and the observed difference between shots in strong and weak material (Figure 5) provide some insights into the generation of explosion *S*-waves. The *Lg*-coda spectral shape's strong dependence on absolute depth

supports explosion *S*-wave generation mechanisms and non-spherical source effects, such ase*Rg*-to-*S* scattering, CLVD, and block motions. From Figure 5, we see that these mechanisms may be quite dependent on the emplacement velocity and density conditions, as well as the scattering properties of the region, such as geologic heterogeneity and topography. For frequencies of 1-3 Hz, these emplacement conditions may add significant uncertainty to resulting *Lg*-coda amplitudes, affecting seismic yield estimation. However, the peaking of the *Lg*-coda spectra offers opportunities to potentially identify unusually shallow events, and may therefore be a useful depth discriminant.

It would be useful to know if *P* and *S*-waves are affected in the same way by emplacement conditions, because differentially affected body waves would have important implications for *P/S* ratio discrimination methods. *Vergino and Mensing* (1990) have used the $m_b(Pn)$ relation to show that emplacement conditions affect *P*-waves, and here we show that emplacement conditions also affect *S*-waves, as seen in the *Lg*-coda to seismic inferred yield relation. Unfortunately, the two methods are different enough to make a meaningful comparison of the effects of emplacement conditions on *P* and *S*-waves impractical. A useful study would look at the effects of emplacement conditions on *P*-waves using newer *P*-coda methods (e.g., *Mayeda*, 2007). It would then be possible to compare the *P*-coda results with the results here, and quantify the differential effects, if any, of emplacement conditions on *P* and *S* coda waves.

In the future, we will further explore the relationship between emplacement depth and spectral peak by looking at pairs of explosions and their subsequent cavity collapses. These pairs would provide controls on location and depth, while allowing magnitude to vary. Since coda measurements average over the source radiation pattern, the difference

between an explosion and its collapse event should have little impact on the coda amplitudes.

CONCLUSIONS

Using the coda methodology, we computed stable, coda-derived spectra from regional recordings for 188 underground nuclear tests at NTS. We find that the explosions exhibit a spectral peak, in sharp contrast to earthquakes from NTS. In general, larger yield events are buried at larger depths for containment purposes, but we find evidence that the frequency of the spectral peak is dependent on emplacement depth, not on inferred yield. For example, the explosions Baseball and Borrego have the same depth and spectral peak, yet their magnitudes and thus inferred yields are very different. A possible mechanism for this observation is *Rg*-to-*S* scattering in the near-source region, perhaps due to near-surface structural complexity, rugged topography, or CLVD. Whichever the dominant cause, this study provides empirical constraints on numerical modeling for NTS explosions (*Myers et al*., 1999, *Gupta et al*., 1992). A summary of our findings are as follows: 1) the coda-derived spectra show a peak which is dependent upon emplacement depth, not yield; 2) inferred yield estimates from the coda are stable and show a dependence upon the near-source strength and gas porosity; 3) for explosions with the same $m_b(Pn)$ or inferred yield, those in weaker material have lower coda amplitudes at 1-3 Hz; 4) for NTS, coda amplitudes between 1-3 Hz for high-strength and low gas porosity provide a lower bound on the inferred yield estimate; 5) the high-frequency spectral decay is steeper for explosions in weak, high-gas-porosity material.

References

Denny, M. D., Taylor, S.R., and Vergino, E.S., 1987, Investigation of mb and Ms formulas for the western United States and their impact on the Ms/mb discriminant, Bull. Seis. Soc. *Am*., **77**, 3, pp. 987-995.

Gupta, I.N., Chan, W.W., and Wagner, R.A., 1992, A comparison of regional phases from underground nuclear explosions at east Kazakh and Nevada Test Sites, *Bull. Seis. Soc. Am*., **82**, 1, pp. 352-382.

Mayeda, K., 1993, mb (Lg Coda): A stable single station estimator of magnitude, *Bull. Seism. Soc. Am*., **83**, 851-891.

Mayeda, K., and Walter, W.R., 1996, Moment, energy, stress drop, and source spectra of western United States earthquakes from regional coda envelopes, *J. Geophys. Res*., **101**, 11,195-11,208.

Mayeda, K., Hofstetter, A., O'Boyle, J.L., and Walter, W.R., 2003, Stable and transportable regional magnitudes based on coda-derived moment-rate spectra, *Bull. Seism. Soc. Am.*, **93**, 1, 224-239.

Mayeda, K., Gök, R., Walter, W.R., and Hofstetter, A., 2005, Evidence for non-constant energy/moment scaling from coda-derived source spectra, *Geophys. Res. Let*., **32,** L10306.

Mayeda, K., 2007, Coda wave methods for explosion monitoring: Recent scaling observations and new methods employing P codas, *Seis. Res. Let*., **78**, 239.

Mayeda, K., Malagnini, L., and Walter, W.R., 2007, A new spectral ratio method using narrow band coda envelopes: Evidence for non-self-similarity in the Hector Mine sequence, *Geophys. Res. Let*., **34**, L11303.

Myers, S.C., Walter, W.R., Mayeda, K., and Glenn, L., 1999, Observations in support of *Rg* scattering as a source for explosion S waves: regional and local recordings of the 1997 Kazakhstan depth of burial experiment, *Bull. Seism. Soc. Am.*, **89**, 2, 544-549.

Myers, S.C., 2007, Numerical experiments investigating the source of explosion S-waves, *Seism. Res. Lett.*, **78**, 2, 240.

Nordyke, M. D., 1962, An analysis of cratering data from desert Alluvium, *J. Geophys. Res.*, **67**, 1965-1974.

Nuttli, O.W., 1986, Yield estimates of Nevada Test Site explosions from seismic Lg waves, *J. Geophys. Res.*, **91**, 2137-2151.

Patton, H.J., 1988, Application of Nuttli's method to estimate yield of Nevada Test Site explosions recorded on Lawrence Livermore National Laboratory's digital seismic system, *Bull. Seism. Soc. Am.*, **78**, 1759-1772.

Patton, H.J., and Taylor, S.R., 1995, Analysis of *Lg* spectral ratios from NTS Explosions: implications for the source mechanisms of spall and the generation of *Lg* waves, *Bull. Seism. Soc. Am.*, **85**, 1, 220-236.

Sammis, C.G., Biegel, R.L., and Johnson, L.R., 2007, Effect of rock damage on seismic waves generated by explosions, *Seism. Res. Lett.*, **78**, 2, 240.

Stevens, J.L., Baker, G.E., and Xu, H., 2007, Constraints on mechanisms for explosion-generated shear waves, *Seism. Res. Lett.*, **78**, 2, 240.

Stevens, J.L., Xu, H., and Baker, G.E., 2006, The physical basis of the explosion source and the generation of regional seismic phases, Proceedings from the 28th Seismic Research Review, 681-692.

Taylor, S. R. and G. E. Randall, 1989. The effects of spall on regional seismograms, *Geophys. Res. Lett.*, 16, 211-214.

Vergino, E.S., and Mensing, R.W., 1990, Yield estimation using regional $m_b(Pn)$, *Bull. Seis. Soc. Am.*, **80**, 3, 656-674.

Walter, W.R., Mayeda, K., and Patton, H.J., 1995, Phase and spectral ratio discrimination between NTS earthquakes and explosions. Part I: Empirical Observations, *Bull. Seis. Soc. Am.*, **85**, 4, 1050-1067.

This work was performed under the auspices of the U.S. Department of Energy by University of California, Lawrence Livermore National Laboratory under Contract W-7405-Eng-48